Heliyon 10 (2024) e39657

Contents lists available at ScienceDirect

Heliyon

journal homepage: www.cell.com/heliyon

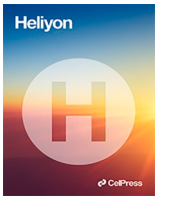

Research article

Optimizing dielectric constants of epoxy composites infused with Palmyra palm and nano fillers using response surface methodology

Suresh Thirupathi [a], Venkatachalam Gopalan [b], Elango Mallichetty [a,*]

[a] School of Mechanical Engineering, Vellore Institute of Technology, Chennai, 600127, Tamilnadu, India
[b] Centre for Advanced Materials and Innovative Technologies, Vellore Institute of Technology, Chennai, 600127, Tamilnadu, India

ARTICLE INFO

Keywords:
Palm fruit fibre
Nanofillers
Dielectric constant
BBD
Response surface methodology

ABSTRACT

The study focuses on Palm fruit Fibers (PF) extracted from the palmyra palm tree (Borassus flabellifer) treated with 5 % alkali solution (NaOH). This treatment eliminates impurities from the fiber surface and enhances bonding with the epoxy matrix. Epoxy composites, reinforced with PF/nanofillers (h-BN, Al_2O_3 and MWCNT), are developed by using the box Behnken method (BBD) and dielectric constant is investigated under high-frequency and electrical field conditions. Dielectric constants (K) of the nanocomposites are determined using various capacitor terminal setups. The electrical properties of the Epoxy/PF nanocomposite, based on fiber content (Wt. %), fiber mesh size (μm) and nanofillers are evaluated using response surface methodology (RSM). Models, predicting nanocomposite dielectric constants, are established, fitting experimental values closely with R^2 nearing 1 and residuals adhering to a normal probability plot. The optimized dielectric constant of 1.05 is achieved at 3 wt% palm fiber content, 150 μm fiber mesh size and 1 wt% nano h-BN.

1. Introduction

Recent attention towards natural fiber composite materials is increased because of their eco-friendly features and economic benefits. The use of natural fibers surpasses that of synthetic materials to strengthen composites and delivers a range of applicability. Palm fiber presents a high potential for diverse applications especially as dielectric material. Palm fiber composites stand out as a suitable solution for constructing remarkable dielectric materials with improved dielectric constant attributes. Investigations showed that the dielectric constant of palm fiber composite elements rises too with more fiber incorporation yet the loss changes with frequency indicating prospects for twistable dielectric uses [1]. The chemical characteristics and water content of palm fibers determine the composites performance. Variations in moisture levels of palm fibers arise from their extraction methods and impact their compatibility with the polymer matrix [2]. Research indicates that palm fibers, losing their hydrophilicity after alkali treatment, improves their compatibility with hydrophobic polymers [3]. An increased bond strength is necessary for enhancing the efficiency with which load transfers from the matrix to the fibers and contributes to improving mechanical properties [4].

The thermal characteristics of composites made from palm fiber surpass their mechanical performance. Studies explored that palm fiber composites effectively decrease thermal conductivity placing them advantageously for use in insulating materials [5,6]. Both

* Corresponding author.
E-mail addresses: sureshthiruppathi11@gmail.com (S. Thirupathi), gopvenki@gmail.com (V. Gopalan), elango101@yahoo.com (E. Mallichetty).

https://doi.org/10.1016/j.heliyon.2024.e39657
Received 3 June 2024; Received in revised form 19 October 2024; Accepted 21 October 2024
Available online 22 October 2024

palm fiber varieties and the procedures followed in production impact the thermal efficiency of these composites [7]. Composites made from date palm fibers excel in thermal diffusivity and effusivity suggesting their effectiveness as green insulation materials in the construction industry [8]. The consequences of using palm fiber composites for the environment are key. Their ability to decompose palm fibers contribute significantly to lessening the carbon footprint associated with synthetic fiber manufacturing. In palm oil regions the repurposing of agricultural waste including empty fruit bunches from oil palms yields substantial benefits. The growth of these innovations matches the trend of employing sustainable resources in both the construction and automotive sectors [9].

Investigation into sustainable materials focused on the use of nanofillers in natural fiber composites for their positive effects on performance. Biodegradable and lightweight materials like hemp and coir are blended into composites. Enhancing the polymer's performance against moisture and poor strength requires adding nanofillers [10,11]. Research shows that carbon nanotubes, graphene and silica boost the strength of natural fiber composites. By incorporating CNTs into the mixture, tensile strength and modulus might be enhanced because of their favourable aspect ratio and outstanding mechanical characteristics [12,13]. When multiple nanofillers are combined, they enhance the adhesion between the fiber and matrix allowing for load transfer and reduced crack creation [14]. It is especially relevant in applications that require high stiffness-to-weight ratios and this is present in automotive and aerospace components [15]. Using natural fibers along with nanofillers brings clear environmental benefits. With increasing focus on sustainable and recycled goods, it is needed to develop hybrid composites utilizing renewable materials that are enhanced by nano engineering. This is in line with the increasing trend of the usage of environmental friendly material across different sectors such as building and construction, automobiles and consumer products [16].

Boron nitride (BN) nanofillers gain significant attention in composite materials because they integrate with natural fiber systems. Combining BN with natural fibers elevates attributes such as thermal conductivity and mechanical resilience and delivers electrical insulation for many purposes in packaging and structural design. Due to its great thermal conductivity, boron nitride becomes a valuable nanofiller. Tests show that BN nanosheets significantly improve the thermal characteristics of polymer composite materials. The heat conductivity of h-BN falls from 2000 to 4000 W/mK range that is perfect for efficient heat transfer applications [17,18]. When blended with natural fibers, this aspect proves useful since they generally have reduced thermal conductivities. When blending BN with natural fibers a composite emerges that can effectively manage heat and stays lightweight like the natural fibers. BN nanofillers significantly enhance the mechanical strength of materials when added to natural fiber composites. Suggestions point to the advantage of incorporating BN to strengthen and toughen materials for structural purposes [19,20]. The flexible shape of BN nanosheets enhances load distributed within the polymer matrix and boosts the composite's strength. BN improves the mechanical performance of epoxy composites to fulfil the requirements of advanced tasks. BN nanofillers increase the electrical insulation of natural fiber composites and simultaneously enhance their thermal and mechanical characteristics. In sectors like electronic packaging and the automotive field, electrical insulation plays a vital role. With a notable bandgap of around 5.5 eV, BN can serve as an insulator efficiently and maintain its thermal management functions. This exceptional characteristic provides vital utilities in building advanced materials that demand insulation from electrical charges along with thermal efficiency.

Adding alumina nanofillers to natural fiber-based composites greatly boosts their conducting nd strength characteristics. Research shows that alumina nanoparticles boost the bond between fibers and the polymer matrix resulting in improved load distribution and increased mechanical strength [21,22]. Alumina's inclusion, raising the tensile and flexural strengths of epoxy composites, is vital for applications with strict mechanical demands [23]. The excellent electrical insulation performance of these composites is improved due to alumina's high dielectric constant in applications requiring electrical or electronic systems [24]. Joining natural fibers with alumina nanofillers enhances their mechanical strength and refines their dielectric properties for advanced engineering use. Using alumina nanofillers in natural fiber composites provides an effective route to increase their overall efficiency [25].

Although the usage of natural fibers are rising in composite materials, the optimization of the dielectric qualities of epoxy composites with alkaline-treated palm fruit fibers combined with advanced nanofillers like hexagonal boron nitride remains understudied. The existing studies are mostly centred on the mechanical and thermal properties instead of the impact of natural fibers and nanofillers on dielectric performance in high-frequency applications. The drive behind this research comes from the increasing demand for environmental friendly materials in the electronic and insulation fields. Using natural fiber composites presents a green choice over synthetics; nevertheless, their effectiveness in electrical use needs additional refinement. This study intends to fulfil the requirement for effective insulators with sustainable low dielectric constant materials by analyzing the dielectric properties of palm fruit fiber composites and adjusting their makeup using the Box-Behnken Design (BBD) technique.

Table 1
Dielectric properties of matrix, reinforcement and nanofillers.

Material	Matrix	Reinforcement	Nanofillers		
	Epoxy	Palm Fiber	MWCNT	h-BN	Al_2O_3
Dielectric Constant	3.05	3 to 8.31	2.5 to 21.6	2.89 to 6.93	9.5
Reference	[30]	[31,32]	[33]	[34]	[35]

2. Experimental methods

2.1. Materials

The study utilizes Epoxy resin LY556 with a density of 1.16 g/cc and the polyamine hardener PA HY951, both sourced from Herenba Instruments & Engineers, Chennai. Palmyra palm fruits are gathered from Chempadu, Tirunelveli, India while h-BN powder (~60 nm 99.9 % Purity) is procured from Nanoshell Pvt.Ltd. Additionally, alumina nanopowder (Al_2O_3 ~20–30 nm 99.9 % Purity) and MWCNT (~10–30 nm 95 % Purity) are obtained from Sisco Research Laboratories Pvt. Ltd, Maharashtra. All chemicals are employed in their original state without undergoing further purification. Dielectric properties of the selected materials are mentioned in Table 1.

2.2. Pre-treatment of fibre

Prior to biocomposites preparation, chopped palm fibers of varying lengths are initially cleansed using distilled water to eliminate surface impurities. Then it is air-dried at room temperature and subsequently is placed in an oven at 90 °C for 4 h to remove any moisture.

Fig. 1 shows the extraction process of the palm fruit fiber from the Palmyra fruit. These palm fruit fibers (PFF) are then immersed in a 5 % NaOH solution by weight for 30 min at room temperature. After the soaking process, the fibers undergo multiple rinses with water to eliminate NaOH residues on the fiber surface. Neutralization is carried out using a 3 % diluted hydrochloric acid (HCl) to remove excess NaOH residues [26,27]. Following neutralization, the fibers are washed again with distilled water and left to air-dry at room temperature for 2 days. Fig. 2 represents the alkaline chemical treatment of the palm fruit fiber to reduce impurities [28].

2.3. PFF composite preparation

The hand layup technique is utilized to fabricate composite material samples comprising PFF and various fillers. Fig. 3 delineates the gradual steps meant for sample fabrication. The next phase involves incorporating filler (h-BN, Al_2O_3, MWCNT) with PFF into the epoxy resin matrix, following the BBD methodology. For each experimental run, epoxy composites are prepared by varying the palm fiber content (A), palm fiber mesh size (B) and nanofiller type (C) according to the design matrix. This mixture is ultrasonicated for 30 min to achieve uniform density and distribution. A consistent 10:1 wt ratio between the resin and hardener is maintained across all models. Subsequently, a silicone rubber mould measuring 50 mm × 50 mm × 10 mm is prepared with suitable tolerance. The palm fiber/filler blend is poured into this mould and left at room temperature for 24 h and eventually it is resulted in rectangle size PFF/filler composites. These sample composites-based BBD variables are prepared and shown Fig. 4. The dielectric constant of the prepared composite materials is measured, and the performance analysis is optimized using the BBD method with Minitab software.

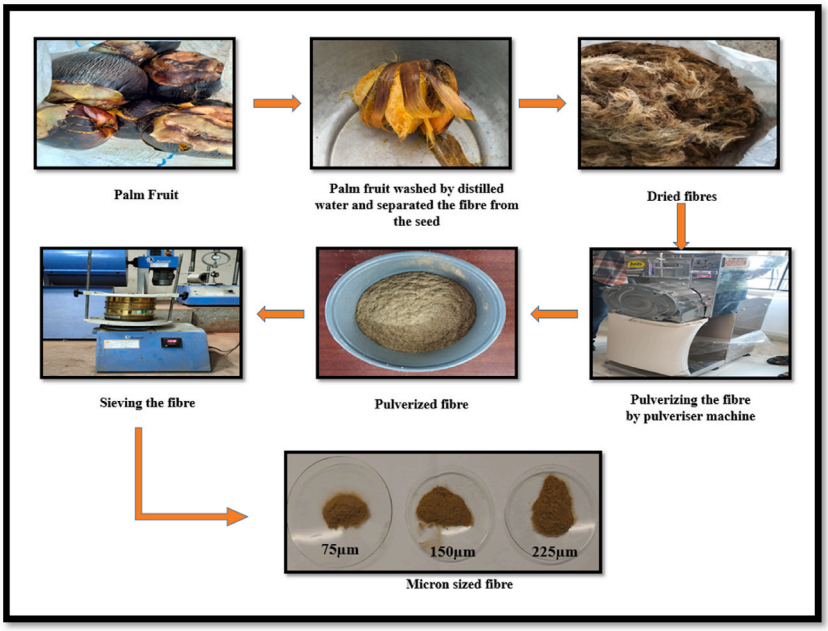

Fig. 1. Extraction process of the Palmyra palm fruit fibre.

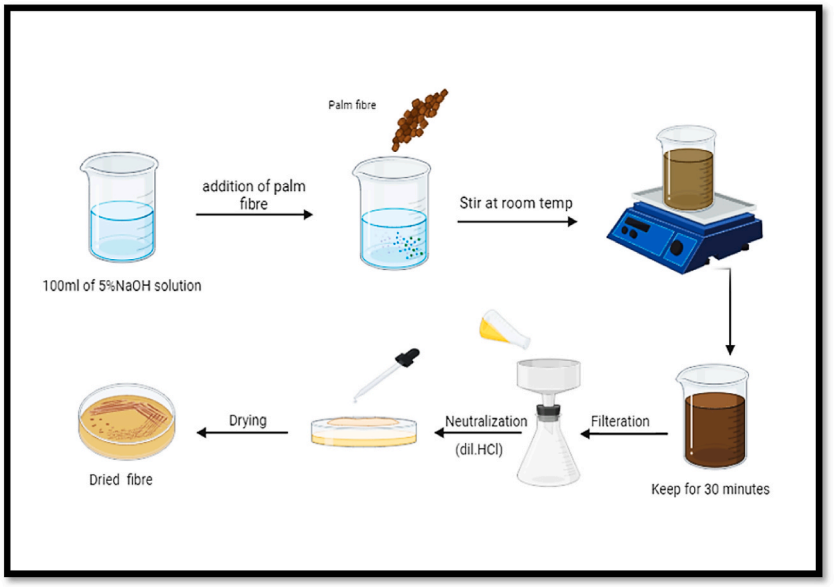

Fig. 2. Chemical treatment of palm fibre.

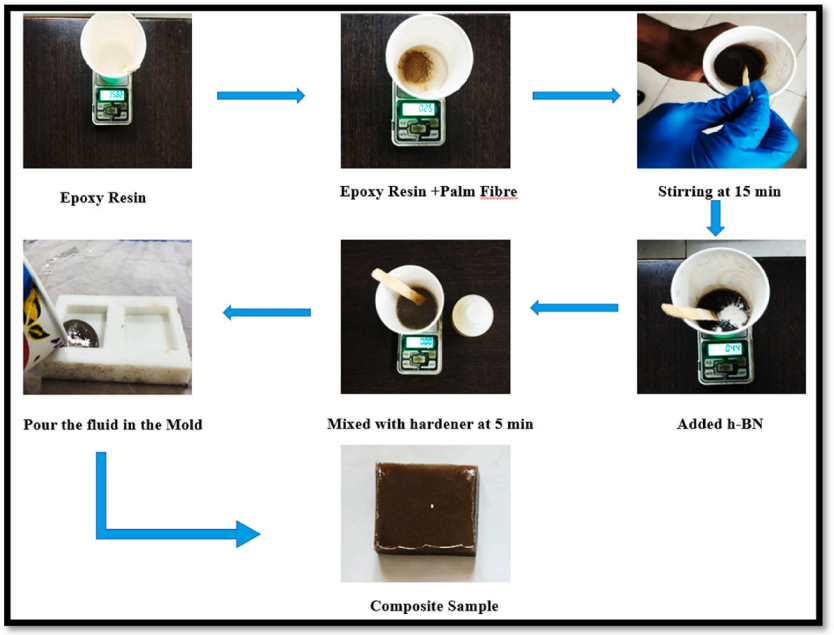

Fig. 3. Step by step process of sample fabrication.

2.4. FTIR analysis

Composite samples selected from the Box-Behnken Design (BBD) are analyzed for FTIR spectra with the FT-IR spectrometer (Shimadzu) to investigate the interaction mechanism between epoxy, palm fiber and nanofillers. FTIR spectra are collected in the wavelength range of 500–4000 cm^{-1}, with each sample subjected to 32 scans at a resolution of 4 cm^{-1}.

2.5. Dielectric constant experiment

The dielectric constant of composite samples is determined using a dielectric constant apparatus as shown in Fig. 5. The apparatus includes variable capacitor terminals on its front panel. Initially it is set at Q1 using a 100 PF standard value, the sensitivity of the

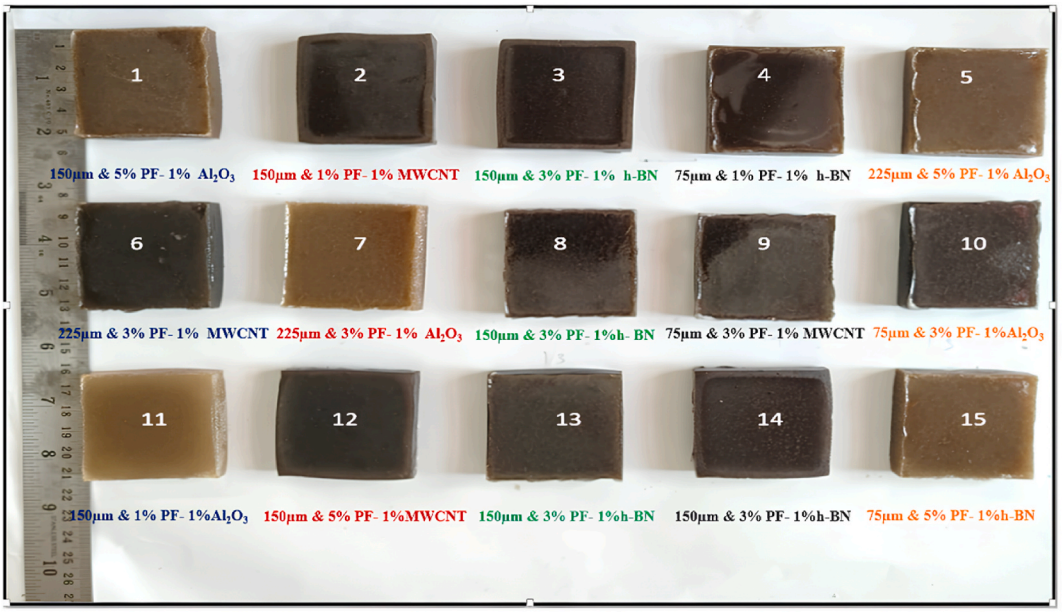

Fig. 4. Fabricated samples as per BBD table.

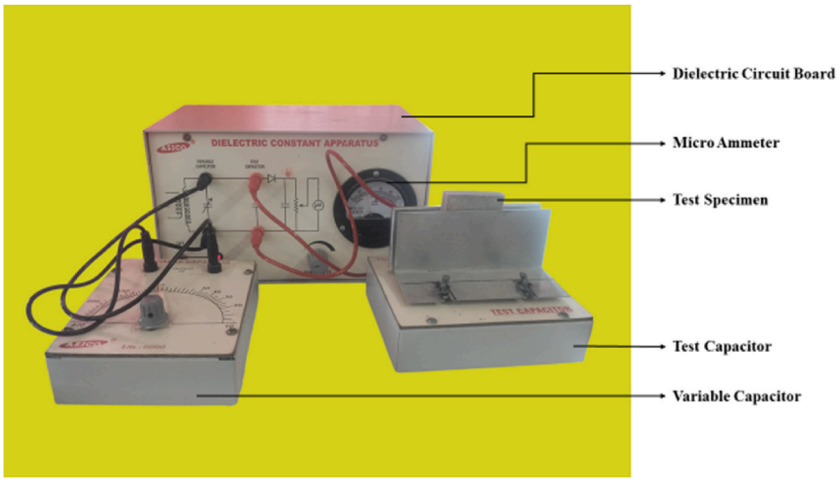

Fig. 5. Dielectric constant apparatus.

control buttons is adjusted to achieve a deflection between 85 and 90 μA. Dielectric constant is measured by inserting the test sample between two metal sheets and the variable capacitor is adjusted until maximum deflection or resonance is reached, noted as Q2. Following sample removal, Q3 is measured under resonance conditions. This sequence is repeated for all samples to calculate the dielectric constant (K) using equation (1) [29].

$$K = \frac{Q1 - Q2}{Q1 - Q3} \tag{1}$$

Where,

Q1 is the capacity of the standard variable capacitor at resonance. Q2 denotes the capacity at resonance when the test capacitor with the sample is present. Q3 refers for the capacity at resonance when the test capacitor is absent from the standard variable capacitor.

3. DOE for response surface methodology (RSM)

BBD is utilized to optimise three variables using RSM. The design matrix and analysis of experimental data are conducted using

Minitab software. Table 2 shows the input parameters that are varied at three levels in the factorial design. Three parameters, included in this study, are filler content (C), fibre content (A) and fibre mesh size (B), each at three levels (coded as −1, 0, +1).

The experimental design, consisted of 15 runs, including three replicates of center points, is to ensure an appropriate quadratic response surface and experimental error estimation. Each run represents a unique combination of the input parameters at different levels. Each component is systematically modified to evaluate both the individual and combined impacts and the arrangement of the design facilitates an efficient exploration of the effects of these parameters on the dielectric constant. While runs 4, 5, 11 and 14 provide more diversity to discover quadratic and interaction effects, runs 1, 2, 3, 6, 7, 9, 10, 12 and 15 involve combinations of the components at different levels. Several centre points (runs 3, 8, 13) are included in the design to ensure an appropriate quadratic response surface and experimental error estimation. Each row in Table 3 represents a unique experimental run by varying the palm fiber %, palm fiber mesh size and nano fillers at different levels according to the experimental design.

All the experimental data, analyzed using Minitab, are on different variables and levels. To efficiently organize the experiments in this scenario involving A, B, C as input data at 3-level factorial, it is normally set up design matrix to plan the experiments efficiently. Furthermore, Analysis of Variance (ANOVA) is performed to determine significant factors and interactions. Response surface analysis is carried subsequently to understand the effects of parameters on the dielectric constant followed by the optimization of process parameters based on the response variable.

A polynomial model with two factors typically represents a simpler relationship between the independent variables A, B, C and the response variable (y). Such a model could be expressed as presented in Equation (2).

$$Y = b_0 + \sum_{i=1}^{k} b_i X_i + \sum_{i=1}^{k} b_{ii} + X_i^2 + \sum_{i>j}^{k} \sum_{i=1}^{k} b_{ij} X_i X_j + \varepsilon \tag{2}$$

From equation (2), Y is the predicted response (Dielectric Constant), b0 is the model constant, bi is the linear coefficient, bii is the quadratic coefficient, bij is the interaction coefficient, Xi is the independent variables and ε is the statistical error.

4. Results and discussions

4.1. Composite samples

The approach used to prepare and characterize palm fruit fiber (PFF) composite is comprehensive. A systematic pre-treatment of fibers is performed, which includes cleaning fibers with distilled water and subsequently thermal treatment at 90 °C for 4h to remove moisture. Fiber quality is improved by chemical treatment using 5 % NaOH solution at 30 min and the fibers are neutralized with 3 % HCl. Composite fabrication by hand layup showed successful results, with several key variables of palm fiber content, mesh size and nanofiller type (h-BN, Al_2O_3, MWCNT). The consistency is maintained in manufacturing process through 30-min ultrasonication for uniform density and a standard 10:1 wt portion resin to hardener. The samples are produced in 50 mm × 50 mm × 10 mm silicone rubber molds and cured at room temperature for 24 h. The palm fibers are integrated with different nanofillers using this systematic approach to create structured composites for further characterization and optimization.

SEM image (Fig. 6) demonstrate a dramatic change in palm fiber morphology after alkali treatment. The untreated fiber begins with a smooth surface due to the wax, lignin and hemicellulose that coat the fiber surface shown in figure (a &c). Substantial structural changes are observed in the fiber after the alkali treatment, the fiber surface becomes rough and pores appear, which can be attributed to the removal of these surface components shown in figure (b&d). Moreover, the exposure of internal fibrils implies the destruction of the outer layers, increasing the fiber's surface area and its interfacial adhesion properties, especially when it is used in a composite material. In addition, this treatment reduces the fiber's natural hydrophilicity, leading to better compatibility with hydrophobic matrices. These changes render the treated palm fiber more suitable for reinforcing applications where the rougher surface and exposed fibrils result in enhanced bonding and load transfer in composite structures. Alkali treatment significantly enhances the potential of palm fiber to be used as an advanced material in reinforcing composites where improved mechanical performance is required.

4.2. Analysis of variance (ANOVA) for dielectric constant

Analyzing variance is a crucial step in evaluating the significance of every component involved in the model, especially when determining each variable influences a response variable, such as the dielectric constant. The p-values of each factor in an ANOVA aid in determining the significance of that factor's impact on the response variable.

Table 2
Factors for Implementation in experimental design.

Variable	Parameter		Level		
	Factor	Unit	−1	0	+1
A	Palm Fiber (PF)Content	%	1	3	5
B	Palm Fiber Mesh Size	μm	75	150	225
C	Nanofiller	%	MWCNT (1)	h-BN (2)	Al_2O_3 (3)

Table 3
Experimental design from Minitab.

Run	Independent Variables					
	Coded Values			Actual Values		
	A	B	C	A	B	C
1	(+1)	0	(+1)	5	150	3
2	(-1)	0	(-1)	1	150	1
3	0	0	0	3	150	2
4	(-1)	(-1)	0	1	75	2
5	(+1)	(+1)	0	5	225	3
6	0	(+1)	(-1)	3	225	1
7	0	(+1)	(+1)	3	225	3
8	0	0	0	3	150	2
9	0	(-1)	(-1)	3	75	1
10	0	(-1)	(+1)	3	75	3
11	(-1)	0	(+1)	1	150	3
12	(+1)	0	(-1)	5	150	1
13	0	0	0	3	150	2
14	(+1)	(-1)	0	5	75	2
15	(-1)	(+1)	0	1	225	2

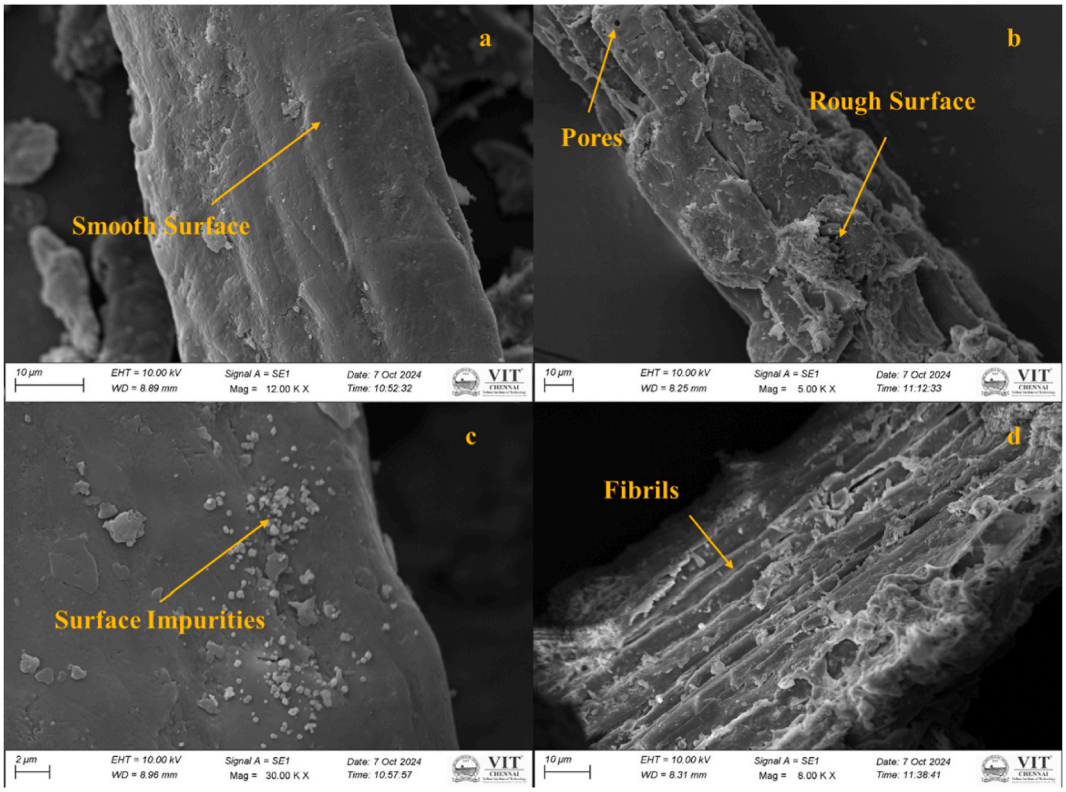

Fig. 6. SEM images of palm fiber before and after alkali treatment: (a&c) Untreated fiber, (b&d) After alkali treatment.

The modified R^2 of 0.9712 and the projected R^2 of 0.8209 have a reasonable coordinate, which makes this result comparable to the results [37,38]. The difference found between the projected R^2 and the modified R^2 is 0.15, falling within the acceptable range (no more than 0.2) for a good model. Sheer examination of R^2 alone is insufficient to determine the goodness of fit because more independent variables can raise R^2. However, adjusted R^2 only increases (or decreases) in the presence of strong correlations between the independent and dependent variables. Contrarily predicted R^2 reveals the complexity of the model and its ability to produce responses for new observations. Therefore, adjusted R^2 and the anticipated R^2 represents as essential metrics for analyzing the goodness of fit in statistical analysis. The significance of the data and models in this study is noteworthy, as all R^2 values are approaching 1.

4.2.1. Model significance

The combined effects of A,B, and C significantly influence the dielectric constant, as shown by the ANOVA Table 3 for the dielectric constant of epoxy composites. Table 4 also shows that the overall model is highly significant, with a P-value of 0. With an adjusted mean square (Adj MS) of 0.01517, an adjusted sum of squares (Adj SS) of 0.13653 and a F-value of 53.47, the model has nine degrees of freedom (DF). These outcomes imply that the selected variables and their interplay are pivotal in determining the dielectric characteristics of the composite materials (see Table 5).

4.2.2. Linear terms

The direct effects of the individual factors are important, but they are not statistically significant at the standard 0.05 level. The linear terms in the model together show a near-significant effect with a P-value of 0.066. With a DF of 1, Adj SS of 0, Adj MS of 0, an F-value of 0 and a P-value of 0.969, the fibre weight % (A) has no discernible effect on the dielectric constant within the linear terms. On the other hand, with an Adj SS of 0.003557, Adj MS of 0.003557, an F-value of 12.54 and a P-value of 0.017, B exhibits a noteworthy influence, underscoring its significance in affecting the dielectric constant. C has an Adj SS of 0.000567, Adj MS of 0.000567, F-value of 2 and P-value of 0.216, suggesting no significant effect.

4.2.3. Square terms

Significant non-linear correlations between the components and the dielectric constant are indicated by the highly significant square terms, which represent the quadratic impacts of the factors, with a P-value of 0. AA has a square term with a DF of 1, Adj SS and Adj MS of 0.015528, F-value of 54.73 and P-value of 0.001, indicating a significant non-linear influence. With an Adj SS of 0.013263, an Adj MS of 0.013263, an F-value of 46.75 and a P-value of 0.001, the square term for fibre mesh size (BB) is also significant. With a substantial non-linear influence on the dielectric constant and an Adj SS and Adj MS of 0.076052, an F-value of 268.07 and a P-value of 0, the square term for fillers (C*C) has the most significance.

4.2.4. Interaction terms

P-value of 0.008 indicates that the interactions between factor combinations have a substantial impact on the dielectric constant. The 2-way interaction terms together demonstrate a significant effect. Adj SS and Adj MS of 0.00165, F-value of 5.82, P-value of 0.061 and an interaction between fibre weight percentage and fibre mesh size (AB) demonstrate a near-significant effect. Adj SS and Adj MS of 0.010282, F-value of 36.24, P-value of 0.002 and fibre weight percentage and fillers (AC) interact in a significant way. However, with an Adj SS of 0.001083, an Adj MS of 0.001083, an F-value of 3.82 and a P-value of 0.108, the interaction between fibre mesh size and fillers (B*C) is not significant.

4.2.5. Error and lack-of-fit

A variable not described by the model is represented by the error term, which has five degrees of freedom, an adjuctive SS of 0.001419 and an adjuctive MS of 0.000284. Although precise significance values are not given, the lack-of-fit term, which has three degrees of freedom and an Adj MS of 0.000473, indicates that the model fits the data. Reflecting the intrinsic variability in the repeated measurements, the pure error term has two degrees of freedom and an Adj MS of 0.

The results of the ANOVA analysis show that the dielectric constant of epoxy composites is greatly influenced by the linear and non-linear effects of fillers, fibre mesh size and fibre weight percentage, as well as by their interactions. The findings, highlighting the significance, are to optimise these variables to provide composite materials with the appropriate dielectric characteristics.

Equation (3) is formulated through analysis and relies on coded factors (+1, 0, and −1) to represent the dielectric constant as

Table 4
Analysis of variance result for dielectric constant.

Source	DF	Adj SS	Adj MS	F-Value	P-Value
Model	9	0.13653	0.01517	53.47	0
Linear	3	0.003938	0.001313	4.63	0.066
A	1	0	0	0	0.969
B	1	0.003557	0.003557	12.54	0.017
C	1	0.000567	0.000567	2	0.216
Square	3	0.111981	0.037327	131.57	0
A*A	1	0.015528	0.015528	54.73	0.001
B*B	1	0.013263	0.013263	46.75	0.001
C*C	1	0.076052	0.076052	268.07	0
2-Way Interaction	3	0.011679	0.003893	13.72	0.008
A*B	1	0.00165	0.00165	5.82	0.061
A*C	1	0.010282	0.010282	36.24	0.002
B*C	1	0.001083	0.001083	3.82	0.108
Error	5	0.001419	0.000284		
Lack-of-Fit	3	0.001419	0.000473	*	*
Pure Error	2	0	0		
Total	14	0.137949			

$R^2 = 0.9897$ Adjusted $R^2 = 0.9712$ Predicted $R^2 = 0.8209$.

Table 5
Validation of predicted results with experiment.

Run No	A (fiber)	B (fiber size)	C (nanofiller)	Dielectric Constant (K)		Error
	(Wt%)	(μm)	(Wt%)	Experimental Values	Regression Values	%
1	5	150	3	1.35	1.34	−0.95
2	1	150	1	1.31	1.32	0.76
3	3	150	2	1.05	1.06	0.57
4	1	75	2	1.19	1.18	−0.79
5	5	225	3	1.32	1.34	1.67
6	3	225	1	1.25	1.26	1.15
7	3	225	3	1.25	1.25	−0.06
8	3	150	2	1.05	1.06	0.57
9	3	75	1	1.27	1.27	−0.02
10	3	75	3	1.32	1.32	−0.14
11	1	150	3	1.22	1.24	1.51
12	5	150	1	1.23	1.22	−0.63
13	3	150	2	1.05	1.06	0.57
14	5	75	2	1.21	1.23	1.25
15	1	225	2	1.19	1.19	−0.21

follows:

Based on A, B and C, regression equation (3) estimates the dielectric constant (K) of epoxy composites. Dielectric constant of 2.1183 is the baseline value and the linear terms' negative coefficients show that increasing the fibre content, mesh size, or filler content separately decreases K. As each factor's level rises, the positive quadratic terms imply deteriorating returns. The variables, that interact, capture the combined effects of filler and fibre content. Positive terms with 0.02454AC indicate an increase in K when filler and fibre content are increased, whereas negative terms with −0.000150AB and −0.000212BC indicate a decrease when mesh size and filler are combined.

$$K = 2.1183 - 0.125A - 0.002674B - 0.6636C + 0.01649A^{*}A + 0.000011B^{*}B + 0.15753C^{*}C - 0.000150A^{*}B + 0.02454A^{*}C - 0.000212B^{*}C \quad (3)$$

Fig. 7, normal probability plots, depicts residuals plotted against dielectric values from the experiments. These plots exhibit straight lines indicating a normal distribution, signifying the reliability of the data. Each diamond point on the plot represents a single composite sample, with known actual dielectric constant values and predicted values by the model. The regression line is black, and it represents a perfect correlation between expected and actual values (i.e., y = x). The model predictions are more accurate as the data points approach this line. The alignment of data points around the line of best fit suggests a significant relationship between expected and measured dielectric constants. This shows that the model accurately represents the link between the input parameters and the composites dielectric constant.

4.3. Effect of processing parameters on the dielectric constant

The outcomes are elucidated through 3D response surface and contour plots derived from the predictive model. These illustrations underscore the substantial impact of all input process parameters on the dielectric constant of the biocomposites.

Fig. 8 illustrates the impact of input parameters on dielectric constant behaviour through 3D surface & 2D contour representations. In Fig. 8 (a), the 3D terrain map demonstrates influence of palm fiber content (Wt.%) and fiber mesh size (μm) on dielectric constant. The figure illustrates the way in which the dielectric constant of the epoxy composite fluctuates with fiber quantity and mesh size. The x-axis represents the fiber content (weight %), the y-axis represents the fiber mesh size (micrometers) and the z-axis represents the dielectric constant. The 3D surface map depicts the interplay between fiber content and mesh size, highlighting the locations where the dielectric constant achieves its optimum value. Notably, reducing the fiber mesh size from 75 to 150 μm decreases the dielectric constant, with a slight increase at 225 μm. additionally, a fiber content range of 1–3 % decreases the constant due to improved epoxy-treated fiber interlocking [39]. The optimal fiber content of 3 % is determined from Fig. 8(b). This contour plot, supplemented the 3D plot by presenting a top-down view, makes it easy to identify the fiber content and mesh size combinations that produce various dielectric constants. The contour lines indicate constant dielectric constants, allowing for a more accurate assessment of the impact of parameter changes on the composite's dielectric properties.

Fig. 9 outlines the effect of fiber material (wt.%) and nanofiller (%) on the dielectric constant. Fig. 8 (a) shows the effect of fiber content and nanofiller type (h-BN, Al_2O_3, MWCNT) on the dielectric constant. The X-axis depicts fiber content, whereas the Y-axis represents various forms of nanofillers. The dielectric constant is displayed on the Z axis. The graph helps to understand the effect of adding different nanofillers at varying fiber contents on the dielectric characteristics of the composite. In Fig. 9(a)'s 3D plot, an increase in fiber content from 1 to 3 % correlates with a decrease in the nanocomposite's dielectric constant, potentially attributed to inadequate fiber-matrix wetting [40]. Fig. 9(b)'s 2D contour plot indicates the lowest dielectric constant at 1 % h-BN and the highest at 1 % Al2O3 concerning fiber content (wt. %). This contour map provides a surface picture of the interactions between fibre content and

nanofillers, making it easier to identify ideal combinations that increase dielectric constant. The contour lines represent constant dielectric values over various fibre content and nanofiller combinations.

Fig. 10 presents the relationship between fiber mesh size (μm) and nanofiller (%) on the dielectric constant. Fig. 9(a) depicts the impact of fibre mesh size and various nanofillers on the dielectric constant. The X-axis shows the size of the fibre mesh, the Y-axis denotes the kind and amount of nanofiller, and the Z-axis measures the dielectric constant. The 3D graph depicts the combined effect of mesh size and nanofiller type on the composite's electrical characteristics, highlighting the parameters that optimise the dielectric constant. In Fig. 10 (a)'s 3D surface plot, variations in nanofiller (%) notably impact the bio nanocomposite's dielectric constant. A decrease in 1 % h-BN improves the constant, contrasting with increases at 1 % CNT and 1 % Al2O3 concerning fiber mesh size. This trend might stem from insulation properties, thermal conductivity of h-BN/epoxy polymer, and their interaction with temperature and mass fraction [41–43]. Fig. 10 (b), a contour plot, depicts the data from Fig. 8(a) in two dimensions. It enables a basic investigation of the way various fibre mesh sizes and nanofiller types interact to create certain dielectric constant values the contour lines aid in determining the precise parameter values required for optimal dielectric performance. An increase in h-BN content initially reduces dielectric constant and losses. Fig. 10(b) indicates the highest dielectric constant at 1 % Al2O3 and the lowest at 1 % h-BN concerning fiber mesh size (μm). All of these figures together show that intricate relationships exist between nanofillers, fibre content and fibre mesh size that affect the epoxy composites' dielectric constant. By visualising various factors that affect the electrical properties of the composite, they aid in the optimization process.

Temperature, humidity, composition and production procedures all have an effect on biocomposites dielectric characteristics [44]. Filler particle size is very important in natural fiber-reinforced composites [45]. According to reported research, wood plastic composites with 150 μm fillers performed best [13].

4.3.1. *Effect of alkali treatment on dielectric constant*

Fibre composites, treated with sodium hydroxide, show a decrease in dielectric constant at all frequencies. Less orientation polarisation, occurred when the fibres become more hydrophobic, is the cause of this decrease. The treatment lowers moisture absorption because fewer polar -OH groups in lignocellulosic fibres likely interact with water molecules. Strong hydrogen bonds make these hydroxyl groups in untreated fibres less reactive early. But sodium hydroxide breaks these connections, making the fibres more reactive and less hydrophilic, which reduces the orientation polarisation even more. As a result, fibres treated with sodium hydroxide have dielectric constant values that are noticeably lower than those of untreated composites [46,47.]].

Treatment with alkaline solutions shows that the composites' resistivity increases while the dielectric constant decreases with an increase in base strength or alkalinity. This effect is connected to a reduction in the number of polar groups that can conduct electricity, which also decreases the effects of polarisation [48].

4.4. *Prediction of optimal conditions*

Optimizing material properties to diminish the dielectric constant involves minimizing fiber weight percentage, fiber size, and nanofillers. Analysis based on Figs. 5, 6, and 7 indicate that achieving a dielectric constant of 1.05 necessitates the use of 3 wt% fiber, a fiber size of 150 μm, and the incorporation of h-BN nanofiller, signifying an optimized configuration. The RSM prioritizes dielectric constant reduction by fine-tuning these key variables. The identification of this precise combination, resulting in a remarkably low dielectric constant, stands as an important achievement in the optimization process.

Optimizing values in any process often correlates with cost-saving and efficiency gains. In this case, achieving the desired dielectric constant at specific values of fiber volume, fiber size, and nanofiller type indicates an efficient configuration that balances performance with cost-effectiveness. Further exploration could involve conducting a cost-benefit analysis to determine the threshold where additional modifications cease to be financially viable or where the gains in dielectric constant no longer justify the increased costs of materials, processing, or time [48].

Chemical treatment of PFF composites enhances dielectric characteristics by stabilising polarisation mechanisms, lowering

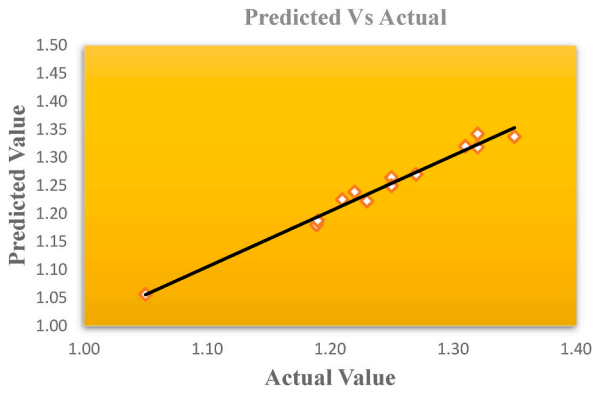

Fig. 7. Residual normal probability plot for Dielectric Constant.

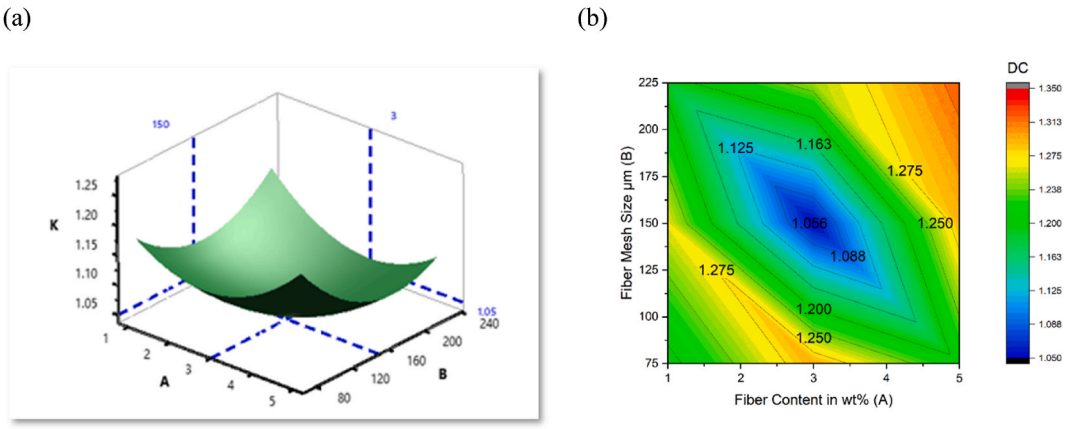

Fig. 8. Surface plot of fibre content vs fibre mesh size on dielectric constant (a) 3D (b) 2D.

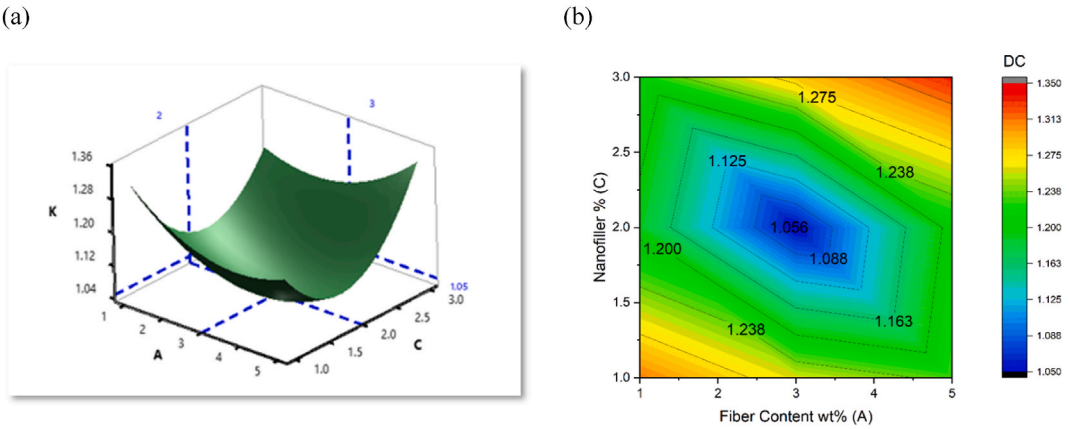

Fig. 9. Surface plot of fibre content vs nanofiller on dielectric constant (a) 3D (b) 2D.

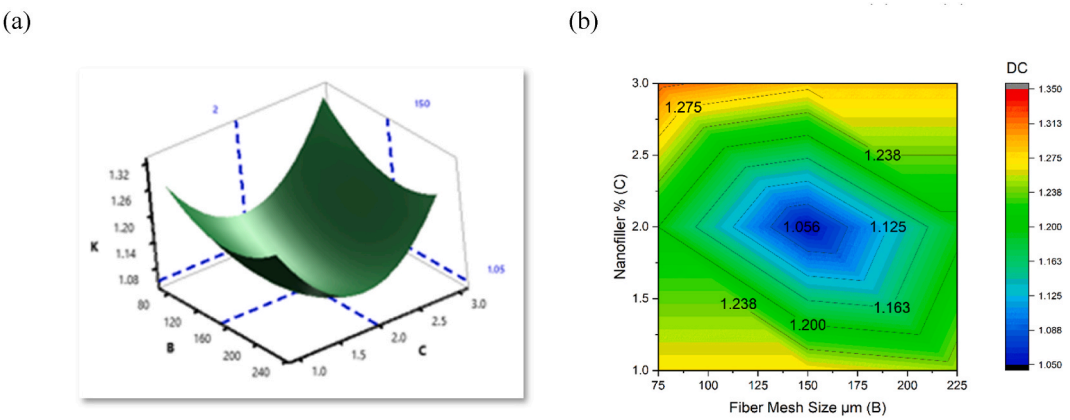

Fig. 10. Surface plot of fiber mesh size vs nanofiller on dielectric constant (a) 3D (b) 2D.

moisture-induced dipolar polarisation and increasing fiber-matrix adhesion. This results in lower dielectric losses and more constant dielectric performance, particularly when combined with insulating nanofillers such as h-BN and Alumina [1&2]. The three factors - fiber content, fibre size and nanofiller type-work synergistically with chemical treatments to optimise the dielectric constant; hence, treated composites are better suited for applications that require significant dielectric stability and low energy loss.

4.5. Standardized effects through Pareto chart

The Pareto chart Fig. 11 shows that nano filler (C) has the greatest impact on the performance of polymer composite materials, implying that optimizing nanofiller content could result in the most significant improvements. The combined parameters of fibre mesh size and nano filler (AC) and fibre mesh size (B) are strongly related, showing that both the physical properties of the fibers and the presence of nanofillers are critical to material performance. The relationships between these parameters, such as fibre mesh size/nano filler (AC) and fibre mesh size/fibre percentage (CC), indicate that a more comprehensive approach to material formulation and processing changes could improve performance even further.

4.6. FTIR analysis of modification effects on composite material

FTIR spectroscopy is a significant technique for characterizing chemical interfaces and interactions within composite materials. Fig. 12 displays the spectrum peaks corresponding to composites 2, 4, 5 and 8 composite sample. The FTIR spectra of epoxy-reinforced natural fiber composites with fillers provides critical understandings into the material's chemical composition and interactions at specific wavenumbers. The 2927 cm-1 peak, typically linked to C-H stretching in methyl (CH3) and methylene (CH2) groups, suggests the presence of aliphatic chains common to both the epoxy and natural fibers. These structures are common in both the epoxy matrix and the natural fibers, specifically in the cellulose and hemicellulose components of the fibers. This peak confirms the integration of the natural fibers within the epoxy matrix [49,50]. The 1603 cm-1 peak could denote the presence of aromatic compounds in the epoxy or its hardeners, or it might indicate lignin in the natural fibers [51,52]. The 1502 cm-1 absorption and characteristic of N-H bending in amides point to amine curing agents in the epoxy or aromatic components in lignin [53,54]. At 1229 cm-1, the C-N stretching in amides or C-O stretching in esters reflects the epoxy's composition and possible ester linkages in the fibers. The presence of these peaks suggests potential interfacial interactions between the epoxy matrix and the natural fibers, which could influence the mechanical and thermal properties of the composite [55,56]. The 1023 cm-1 peak, is indicative of C-O stretching in cellulose. Finally, the 822 cm-1 band is likely due to C-H bending in aromatic structures, which could come from both the epoxy and the natural fibers. According to existing literature, the branches and leaves of palm trees exhibit a higher cellulose content compared to lignin and hemicellulose. Additionally, the lignin and hemicellulose present that they are more amorphous compared to cellulose [50].

4.7. Validation and enhancement of the model

The primary objective of the effective plot for parameters A, B, and C, illustrated in Fig. 13(a), is to comprehend the impact of each constraint on the dielectric constant. An amalgamation of intermediate BN/Palm fiber content and moderate-sized palm fiber particles yields the lowest dielectric constant. Conversely, both slighter and greater content results in the maximum dielectric constant, indicating lower resistance to electric current. The dielectric constant exhibits an inverse relationship with the material's resistance against electric shock. Achieving effective insulation requires identifying the most influential content for each parameter that aligns with composite desirability, resulting in a lower dielectric constant, as outlined in Table 6. Similarly, an optimal content, such as 3.10 wt % of palm fiber, 164.39 μm of palm fiber, and 1 wt % of nano h-BN filler, demonstrates the minimum dielectric constant, as depicted in the optimization plot in Fig. 13(b). The error, calculated between the experimental and optimized combinations, is presented in Table 7, indicating a minimal 1.86 % error. This underscores the achievement of the minimum dielectric constant with the 3/2/2 content corresponding to palm fiber (A)/Mesh size of Palm fiber (B)/filler (C) for the run number of samples 3/8/13.

4.8. Exploring dielectric constants: A Comparative analysis of composite materials

The dielectric constant, found in the present work, is compared with previous polymer composite material research as mentioned in Table 8. Epoxy nanocomposites contain lower dielectric constants, which makes them appropriate for use in electronic components and insulating materials when lower permittivity values are required [70]. Applications requiring improved dielectric characteristics in epoxy polymer composite materials may benefit from polymer nanocomposites with low dielectric constant fillers improving their dielectric response [71] [72].

The properties of composite materials particularly in electronics and insulation heavily depend on their dielectric constant. An analysis of epoxy-reinforced palm fruit fiber composites with hexagonal boron nitride (h-BN) is performed against different polymer composites. This work indicates a dielectric constant of 1.05 for the epoxy/palm fruit fiber/h-BN composite which is considerably lower than various materials listed in the analysis. Earlier examination reveals that nanocomposites derived from epoxy frequently generate diminished dielectric properties. Thus, this trend supports their application in contexts seeking minimal permittivity including insulators and electronic components.

A dielectric constant of 1.143 is recorded for an epoxy composite enhanced with banana fiber and boron nitride (BN). The transformations show the important effect of reinforcing and filler materials on the dielectric characteristics of polymer composites. Adding h-BN fillers with a low dielectric constant enhances the composite's ability in dielectric uses. Using high dielectric materials such as PVDF along with barium titanate silver in composites demonstrates enhanced dielectric properties up to 19.4 and serves for advanced capacitor applications. Composites derived from epoxy with inorganic stone powder possess dielectric properties that can reach 50 making them viable options for high demand dielectric needs. Unlike other options in its class, the current composite displays a lower dielectric constant; hence it is an optimal choice for low-dielectric applications. Findings demonstrate that fibers derived from nature such as palm fruit fiber can be integrated with novel fillers like h-BN to generate efficient and green composite materials.

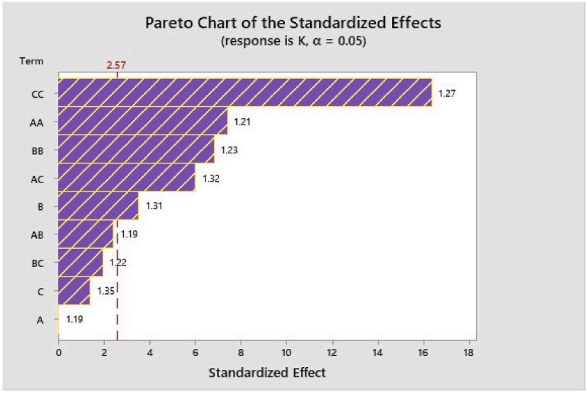

Fig. 11. Pareto Chart of the standardized effects.

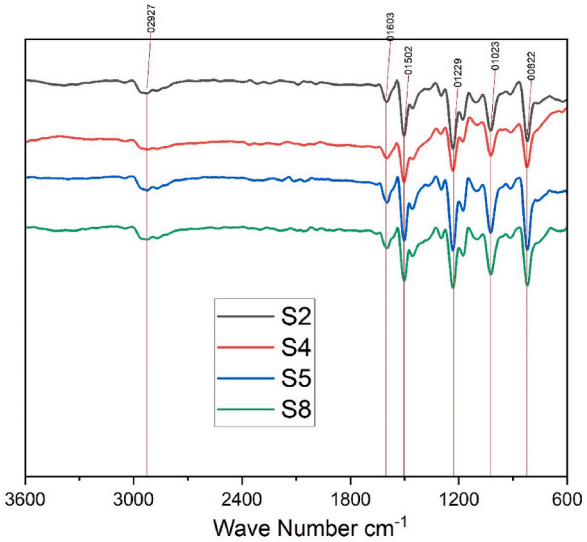

Fig. 12. FTIR spectra of samples 2,4,5 and 8.

The findings show that the epoxy/palm fiber/h-BN composite performs well in low dielectric applications. The current situation represents a common characteristic of polymer nanocomposites as the selection of fillers and reinforcements can change dielectric characteristics. Molecular interactions can be the focus of future studies to clarify diverse fibers and fillers influencing the dielectric behaviour of the composites. This composite, mentioned in this study, reveals a significantly reduced dielectric constant that improves its fit for low dielectric use. Natural fibers like palm fruit fiber can produce high-performance eco-friendly composite materials when enhanced with advanced fillers such as h-BN according to the findings. The epoxy/palm fruit fiber/h-BN composite satisfies the criteria for low-dielectric applications as shown in this study. This highlights the common trend among polymer nanocomposites illustrating thoughtful choice of reinforcements and fillers modifying dielectric traits for particular uses. Extended exploration can investigate the mechanisms occurring at the molecular scale to appreciate several fibers and fillers modifying the dielectric properties of the composites.

5. Conclusion

This research examines the dielectric properties of epoxy composites strengthened by alkali-treated palm fruit fibers and nanofillers using BBD optimization. The investigation focuses on palm fibers and nanofillers influence on the composite's dielectric constant. A dielectric constant of 1.05 is achieved with 3 % palm fiber and a 150 μm mesh size along with 1 % h-BN nanoparticles. Better connections resulting from chemical processes between the fibers and the matrix lead to a decrease in the dielectric constant. After undergoing alkali treatment, the palm fibers become less hydrophilic leading to low moisture absorption and improved bond with the epoxy matrix. Improved attachment strengthens the composite and diminishes its dielectric and loss features to make the composite as an insulator in the electronics field. An assessment test confirms the model's ability to predict correctly with a slight error of 1.86 %

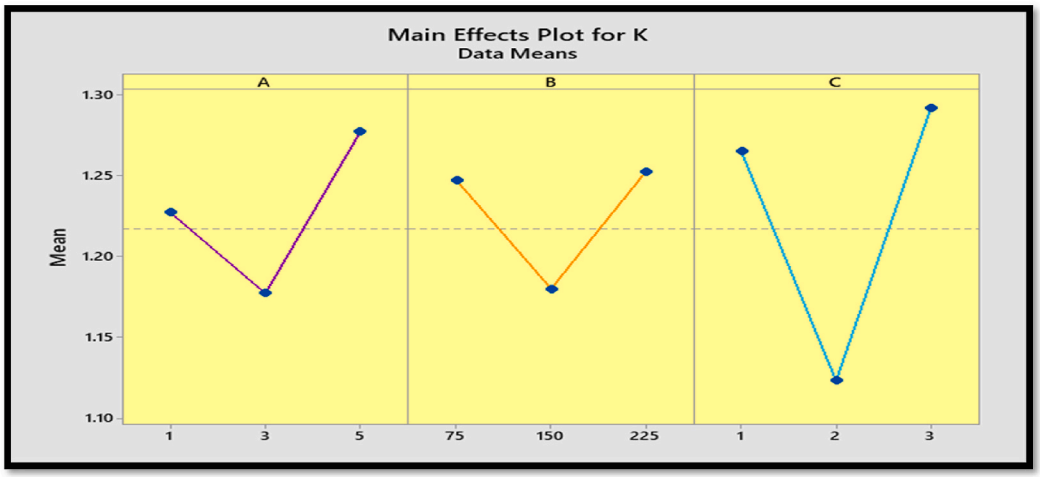

(a)

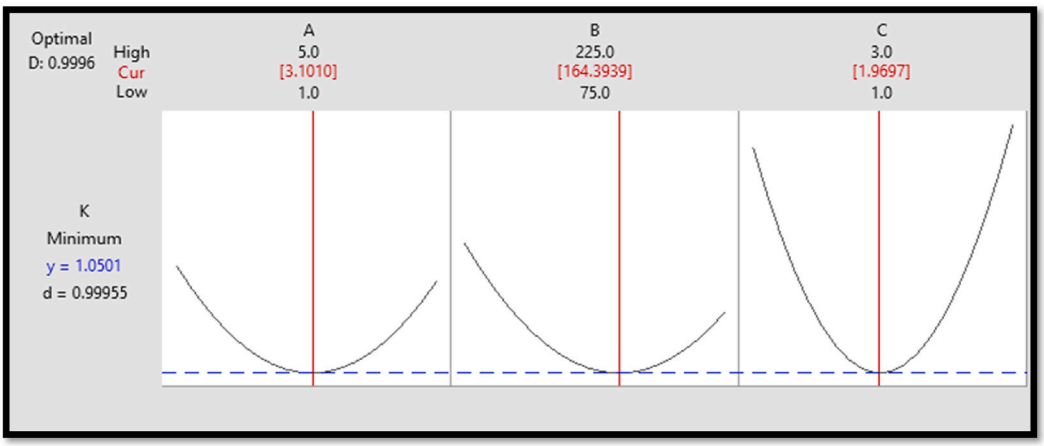

(b)

Fig. 13. (a) Main effect Plot (b) Response optimizer.

Table 6
Objective for optimization Parameters.

Response	Goal	Lower	Target	Upper	Weight	Importance
K	Minimum		1.05	1.35	1	1
Solution	A	B	C	K Fit	Composite Desirability	
1	3.10	164.39	1.96	1.05	0.99	

Table 7
Comparative analysis of dielectric constant: Optimized versus experimental results.

S.No	PF Wt.%	PF Mesh Size μm	Type of Filler Wt.%	Dielectric constant	Error %
1	3.10	164.394	h-BN (1 %)	1.07 (Experimentation)	1.86
2	3.10	164.394	h-BN (1 %)	1.05 (Optimization)	

Table 8
Dielectric properties of polymer composites: A comparative analysis.

S. No	Matrix	Reinforcement	Chemical Treatment	Filler	Dielectric Constant	Reference
1.	Epoxy	Palm Fruit Fibre	Alkaline	h-BN	1.05	Present Work
2.	Epoxy	Banana Fibre	–	BN	1.143	[57]
3.	PVC	Coir Powder	Silane	–	2.256	[29]
4.	Polyester	Jute/Bamboo	Alkaline	–	~3.9	[46]
5.	Polyester	–	–	–	3.3	[58]
6.	HDPE	Coconut fibre	–	Copper Powder	1.43	[58]
7.	PLA	Coconut fibre	–	Copper Powder	1.82	[58]
8.	Natural rubber	Sisal/Coir fibers	Combined Alkaline and Permanganate	–	2.7–3.55	[59]
9.	PVDF	–	–	barium titanate@silver	19.4	[60]
10.	Epoxy	Caryota urens woven	–	coconut husk biochar	5.6	[61]
11.	Polyimide/silsesquioxane composite films	–	–	–	2.28–2.42	[62]
12.	Epoxy	–	–	Inorganic stone waste powder	50	[63]
13.	Epoxy	Aloevera fiber	–	peanut shell biochar	2.3	[64]
14.	Epoxy	Coir and Luffa Cylindrica Fiber	Alkaline	$CaCO_3$	3–4	[65]
15.	polyester	*Hibiscus sabdariffa*	Grafted with ethyl acrylate and acrylonitrile	–	1–7.5	[66]
16.	Epoxy	chicken feather/E-glass	–	–	3.4–5.4	[67]
17.	Epoxy	Palm sugar	Alkaline	–	8–24	[36]
18.	Rubber	Oil palm	NaOH, silane	–	3.2–10.5	[68]
19.	Polypropylene	Flax	Acetylation	–	2.5–18	[69]
20.	Phenol formaldehyde	Banana	NaOH, silane, acetylation, cyanoethylation	–	4–33	[70]

with the experiment.

An essential area for future research involves examining the ecological consequences of incorporating natural fibers and biodegradable matrices into these composites. Determining the life cycle and degradability of these composites is vital for fostering their use in environmental friendly projects. The pairing of advanced nanofillers including h-BN with natural fibers such as palm fruit fiber offers a chance to design sustainable composites that excel in performance and cater to individual industrial requirements. The project lays a foundation for new breakthroughs in crafting dielectric substances with adjustable characteristics suited for particular applications.

CRediT authorship contribution statement

Suresh Thirupathi: Writing – original draft, Resources, Investigation, Formal analysis, Data curation. **Venkatachalam Gopalan:** Supervision, Resources, Project administration, Conceptualization. **Elango Mallichetty:** Visualization, Methodology.

Data availability

Data will be made available on request.

Ethical approval

The manuscript meets all applicable standards about the ethics of experimentation and research, and there is no duplicate publication, fraud, plagiarism, or concerns about animal or human experimentation.

Consent

I, Elango Mallichetty, give my consent for the publication of the Research article.

Funding details

There is no Funding available for this research article.

Declaration of competing interest

The authors declare that they have no known competing financial interests or personal relationships that could have appeared to influence the work reported in this paper.

Acknowledgements

The authors acknowledge the support from the Vellore Institute of Technology, Chennai.

References

[1] B. Neher, et al., Fabrication and optical characterization of palm fiber reinforced acrylonitrile butadiene styrene based composites: band gap studies, Mater. Sci. Appl. 9 (2) (2018) 246–257.
[2] D. Atalie, R.K. Gideon, Extraction and characterization of Ethiopian palm leaf fibers, Research Journal of Textile and Apparel 22 (1) (2018) 15–25.
[3] W. Fatra, et al., Alkaline treatment of oil palm frond fibers by using extract of oil palm EFB ash for better adhesion toward polymeric matrix, Journal of Engineering and Technological Sciences 47 (5) (2015) 498–507.
[4] D. Riyapan, S.A. Riyajan, P. Tangboriboonrat, Preparation of polymer composite: low natural rubber, cassava starch and palm fiber, Adv. Mater. Res. 844 (2013) 314–317.
[5] I. Amara, et al., Experimental study on thermal properties of bio-composite (gypsum plaster reinforced with palm tree fibers) for building insulation, International Journal of Heat and Technology 35 (3) (2017) 576–584.
[6] A. Braiek, et al., Estimation of the thermophysical properties of date palm fibers/gypsum composite for use as insulating materials in building, Energy Build. 140 (2017) 268–279.
[7] S. Benaniba, et al., Thermo-mechanical characterization of a bio-composite mortar reinforced with date palm fiber, Journal of Engineered Fibers and Fabrics 15 (2020) 155892502094823.
[8] R. Boubaaya, et al., Impact of the loading of date palm fibers on the performances of mortars, Rem - International Engineering Journal 76 (2) (2023) 159–168.
[9] M. Alhijazi, et al., Recent developments in palm fibers composites: a review, J. Polym. Environ. 28 (12) (2020) 3029–3054.
[10] M.S. Rabbi, et al., Effect of nano-filler on the manufacturing and properties of natural fiber-based composites: a review, Journal of Engineering Advancements (2023) 101–115.
[11] M.Y. Raghu, G. Goud, Tribological properties of calotropis procera natural fiber reinforced hybrid epoxy composites, Appl. Mech. Mater. 895 (2019) 45–51.
[12] L. Luo, et al., Synergistic “anchor” effect of carbon nanotubes and silica: a facile and efficient double-nanocomposite system to reinforce high-performance polyimide fibers, Ind. Eng. Chem. Res. 58 (36) (2019) 16620–16628.
[13] Z. Wang, et al., Effect of high aspect ratio filler on dielectric properties of polymer composites: a study on barium titanate fibers and graphene platelets, IEEE Trans. Dielectr. Electr. Insul. 19 (3) (2012) 960–967.
[14] H. Radshad, H. Khoramishad, R. Nazari, The synergistic effect of hybridizing and aligning graphene oxide nanoplatelets and multi-walled carbon nanotubes on mode-I fracture behavior of nanocomposite adhesive joints, Proceedings of the Institution of Mechanical Engineers Part L Journal of Materials Design and Applications 236 (9) (2022) 1764–1776.
[15] R. Sundarakannan, et al., Importance of fiber-/nanofiller-based polymer composites in mechanical and erosion performance: a review, J. Nanomater. 2023 (2023) 1–16.
[16] T. Raja, et al., Mechanical properties of banyan fiber-reinforced sawdust nanofiller particulate hybrid polymer composite, J. Nanomater. 2022 (1) (2022).
[17] Z. Su, et al., Fabrication of thermal conductivity enhanced polymer composites by constructing an oriented three-dimensional staggered interconnected network of boron nitride platelets and carbon nanotubes, Acs Applied Materials & Interfaces 10 (42) (2018) 36342–36351.
[18] G. Yun, et al., Strategic fabrication of robust spherical hexagonal boron nitride particles for thermally conductive applications, Acs Applied Engineering Materials 1 (12) (2023) 3359–3367.
[19] W. Cai, et al., Facile fabrication of organically modified boron nitride nanosheets and its effect on the thermal stability, flame retardant, and mechanical properties of thermoplastic polyurethane, Polym. Adv. Technol. 29 (9) (2018) 2545–2552.
[20] S. Wang, et al., Preparation and properties of epoxy composites with multi-scale BN sheets, Appl. Sci. 12 (12) (2022) 6171.
[21] T.K. Patnaik, S.S. Nayak, Investigation of physico-mechanical and thermo-mechanical analysis of alumina filled needle-punch nonwoven jute epoxy composites, Polym. Compos. 39 (5) (2016) 1553–1561.
[22] D.G. Pinto, et al., Mechanical properties of epoxy nanocomposites using alumina as reinforcement - a review, J. Nano Res. 30 (2015) 9–38.
[23] G. Brown, F. Ellyin, Mechanical properties and multiscale characterization of nanofiber–alumina/epoxy nanocomposites, J. Appl. Polym. Sci. 119 (3) (2010) 1459–1468.
[24] N. Dedruktip, W. Leelawanachai, N. Tangboriboon, Natural rubber-whisker alumina fiber composite materials for mechanical and thermal insulation applications, Key Eng. Mater. 789 (2018) 221–225.
[25] A. Amjad, et al., A review investigating the influence of nanofiller addition on the mechanical, thermal and water absorption properties of cellulosic fibre reinforced polymer composite, J. Ind. Textil. 51 (1_suppl) (2021) 65S–100S.
[26] N. Shanmugasundaram, I. Rajendran, Characterization of raw and alkali-treated mulberry fibers as potential reinforcement in polymer composites, J. Reinforc. Plast. Compos. 35 (7) (2016) 601–614.
[27] N. Shanmugasundaram, I. Rajendran, T. Ramkumar, Characterization of untreated and alkali treated new cellulosic fiber from an Areca palm leaf stalk as potential reinforcement in polymer composites, Carbohydrate Polymers 195 (2018) 566–575.
[28] D. Tishkevich, et al., Electrochemical deposition regimes and critical influence of organic additives on the structure of Bi films, J. Alloys Compd. 735 (2018) 1943–1948.
[29] S. Aravindh, G. Venkatachalam, Investigations on dielectric constant of coir powder-reinforced PVC composites, J. Nat. Fibers 20 (2) (2023) 2239501.
[30] T.T.M. Phan, et al., Enhancement of polarization property of silane-modified BaTiO3 nanoparticles and its effect in increasing dielectric property of epoxy/BaTiO3 nanocomposites, J. Sci.: Advanced Materials and Devices 1 (1) (2016) 90–97.
[31] S. Phadke, et al., Dielectric response of Borassus flabellifier wood at different moisture content, Adv. Mater. Res. 347 (2012) 1488–1493.
[32] S. Shinoj, R. Visvanathan, S. Panigrahi, Towards industrial utilization of oil palm fibre: physical and dielectric characterization of linear low density polyethylene composites and comparison with other fibre sources, Biosyst. Eng. 106 (4) (2010) 378–388.
[33] M.M. Altarawneh, The dielectric properties of silicone-multiwall carbon nanotubes nanocomposite in the frequency range from 0.5 to 20 GHz, AIP Adv. 14 (3) (2024).
[34] A. Laturia, M.L. Van de Put, W.G. Vandenberghe, Dielectric properties of hexagonal boron nitride and transition metal dichalcogenides: from monolayer to bulk, npj 2D Materials and Applications 2 (1) (2018) 6.
[35] Y. Thakur, et al., Enhancement of the dielectric response in polymer nanocomposites with low dielectric constant fillers, Nanoscale 9 (31) (2017) 10992–10997.
[36] I.G.N.N. Santhiarsa, A. Sonief, E. Marsyahyo, Effects of alkali treatment and weight fraction on electrical properties of palm sugar fibre-epoxy composite, Contemp Eng Sci 7 (19) (2014) 907–914.
[37] M. Adamu, M.R. Rahman, S. Hamdan, Formulation optimization and characterization of bamboo/polyvinyl alcohol/clay nanocomposite by response surface methodology, Compos. B Eng. 176 (2019) 107297.

[38] B. Chieng, N. Ibrahim, W.W. Yunus, Optimization of tensile strength of poly (lactic acid)/graphene nanocomposites using response surface methodology, Polym.-Plast. Technol. Eng. 51 (8) (2012) 791–799.
[39] P.E. Imoisili, et al., Effect of chemical treatment on the morphology and mechanical properties of plantain (Musa paradisiaca) fiber, IOSR J. Appl. Chem. 10 (5) (2017) 70–73.
[40] M.Z. Hassan, et al., Optimization of tensile behavior of banana pseudo-stem (Musa acuminate) fiber reinforced epoxy composites using response surface methodology, J. Mater. Res. Technol. 8 (4) (2019) 3517–3528.
[41] Y. Tang, et al., Temperature effects on the dielectric properties and breakdown performance of h-BN/epoxy composites, Materials 12 (24) (2019) 4112.
[42] C. Zhang, G.C. Stevens, Dielectric properties of boron nitride filled epoxy composites, in: 2006 IEEE Conference on Electrical Insulation and Dielectric Phenomena, IEEE, 2006.
[43] X. Huang, P. Jiang, T. Tanaka, A review of dielectric polymer composites with high thermal conductivity, IEEE Electr. Insul. Mag. 27 (4) (2011) 8–16.
[44] I. Elloumi, et al., Dielectric properties of wood-polymer composites: effects of frequency, fiber nature, proportion, and chemical composition, Journal of Composites Science 5 (6) (2021) 141.
[45] A. Azlan, et al., A study of dielectric constant and loss tangent of Leucaena Leucocephala wood plastic composite (WPC) substrate, in: 2013 IEEE Symposium on Wireless Technology & Applications (ISWTA), IEEE, 2013.
[46] E. Jayamani, et al., Comparative study of dielectric properties of hybrid natural fiber composites, Procedia Eng. 97 (2014) 536–544.
[47] G. George, et al., Dielectric behaviour of PP/jute yarn commingled composites: effect of fibre content, chemical treatments, temperature and moisture, Compos. Appl. Sci. Manuf. 47 (2013) 12–21.
[48] S. Gopalakannan, T. Senthilvelan, Application of response surface method on machining of Al–SiC nano-composites, Measurement 46 (8) (2013) 2705–2715.
[49] S. Rizal, et al., Interfacial compatibility evaluation on the fiber treatment in the Typha fiber reinforced epoxy composites and their effect on the chemical and mechanical properties, Polymers 10 (12) (2018) 1316.
[50] R.B. Alsuwait, et al., Recent development in the processing, properties, and applications of epoxy-based natural fiber polymer biocomposites, Polymers 15 (1) (2022) 145.
[51] X. Zhang, et al., Method for automatically identifying spectra of different wood cell wall layers in Raman imaging data set, Anal. Chem. 87 (2) (2015) 1344–1350.
[52] N. Zhu, D. Wu, Label-free visualization of fruit lignification: Raman molecular imaging of loquat lignified cells, Plant Methods 14 (1) (2018).
[53] L. Zhao, et al., Accelerated-curing epoxy structural film adhesive for bonding lightweight honeycomb sandwich structures, J. Appl. Polym. Sci. 140 (6) (2022).
[54] T.-Y. Yung, et al., Reinforcement of epoxy resin by additives of amine-functionalized graphene nanosheets, Coatings 11 (1) (2020) 35.
[55] R. Ghumara, P.P. Adroja, P.H. Parsania, Synthesis and physicochemical studies of jute and glass composites of styrenated vinyl esters of multifunctional epoxy resin containing S-triazine ring, Polym. Compos. 37 (1) (2014) 279–287.
[56] M. Shen, M.L. Robertson, Degradation behavior of biobased epoxy resins in mild acidic media, ACS Sustain. Chem. Eng. 9 (1) (2020) 438–447.
[57] D.R. Salunke, V. Gopalan, Investigation of electrical resistance and dielectric constant of Boron Nitride and Banana fiber reinforced epoxy polymer matrix composite, Polym. Polym. Compos. 30 (2022) 09673911221122328.
[58] E. Jayamani, G.A. Nair, K. Soon, Investigation of the dielectric properties of natural fibre and conductive filler reinforced polymer composites, Mater. Today: Proc. 22 (2020) 162–171.
[59] A. Haseena, G. Unnikrishnan, G. Kalaprasad, Dielectric properties of short sisal/coir hybrid fibre reinforced natural rubber composites, Compos. Interfac. 14 (7–9) (2007) 763–786.
[60] Y.-s. Zhang, et al., Heterogeneous BaTiO3@ Ag core-shell fibers as fillers for polymer dielectric composites with simultaneously improved dielectric constant and breakdown strength, Compos. Commun. 27 (2021) 100874.
[61] P. Prabhu, et al., Mechanical, tribology, dielectric, thermal conductivity, and water absorption behaviour of Caryota urens woven fibre-reinforced coconut husk biochar toughened wood-plastic composite, Biomass Conversion and Biorefinery 14 (1) (2024) 109–116.
[62] Y. Ma, et al., Facile strategy for low dielectric constant polyimide/silsesquioxane composite films: structural design inspired from nature, J. Mater. Sci. 56 (2021) 7397–7408.
[63] R. Sahu, et al., Moisture resistant stones waste based polymer composites with enhanced dielectric constant and flexural strength, Compos. B Eng. 182 (2020) 107656.
[64] N. Balaji, et al., Annealed peanut shell biochar as potential reinforcement for aloe vera fiber-epoxy biocomposite: mechanical, thermal conductivity, and dielectric properties, Biomass Conversion and Biorefinery 14 (3) (2024) 4155–4163.
[65] D. Mohana Krishnudu, et al., Influence of filler on mechanical and di-electric properties of coir and luffa cylindrica fiber reinforced epoxy hybrid composites, J. Nat. Fibers 19 (1) (2022) 339–348.
[66] D. Pathania, D. Singh, D. Sharma, Electrical properties of natural fiber graft co-polymer reinforced phenol formaldehyde composites, Optoelectronics and Advanced Materials-Rapid Communications 4 (July 2010) (2010) 1048–1051.
[67] M. Zhan, R.P. Wool, J.Q. Xiao, Electrical properties of chicken feather fiber reinforced epoxy composites, Compos. Appl. Sci. Manuf. 42 (3) (2011) 229–233.
[68] C. Santulli, et al., Influence of content and diameter of fibres and chemical treatment on the dielectric properties of oil palm fibres-rubber composites, Sci. Eng. Compos. Mater. 16 (2) (2009) 77–88.
[69] A. Korneliusz Bledzki, et al., Biological and electrical resistance of acetylated flax fibre reinforced polypropylene composites, Bioresources 4 (1) (2009).
[70] S. Joseph, S. Thomas, Electrical properties of banana fiber-reinforced phenol formaldehyde composites, J. Appl. Polym. Sci. 109 (1) (2008) 256–263.